Available online at www.sciencedirect.com
ScienceDirect
Biosensors and Bioelectronics 23 (2008) 811–819
BIOSENSORS & BIOELECTRONICS
www.elsevier.com/locate/bios

Reversible transition of extracellular field potential recordings to intracellular recordings of action potentials generated by neurons grown on transistors

Ariel Cohen [a], Joseph Shappir [b], Shlomo Yitzchaik [c], Micha E. Spira [a,*]

[a] *Department of Neurobiology, The Life Sciences Institute, The Hebrew University of Jerusalem, Jerusalem 91904, Israel*
[b] *School of Engineering, The Hebrew University of Jerusalem, Jerusalem 91904, Israel*
[c] *Department of Inorganic and Analytical Chemistry, The Hebrew University of Jerusalem, Jerusalem 91904, Israel*

Received 17 May 2007; received in revised form 15 August 2007; accepted 31 August 2007
Available online 12 September 2007

Abstract

The employment of standard CMOS technology to produce semiconductor chips for recording neuronal activity or for its future use to link neurons and transistors under *in vivo* conditions, suffers from a low signal to noise ratio. Using *Aplysia* neurons cultured on CMOS floating gate field effect transistors, we report here that minor mechanical pressure applied to restricted neuronal compartment that face the sensing pad induces two independent alterations: (a) increase in the seal resistance formed between the neuron's membrane and the sensing pad, and (b) increase the conductance of the membrane patch that faces the sensing pad. These alterations (from ∼0.5 to ∼1.2 MΩ and 75 to ∼600 nS correspondingly), are sufficient to transform the low capacitive coupling between a neuron and a transistor to Ohmic coupling, which is manifested by semi-intracellular recordings of APs with amplitudes of up to 30 mV. The semi-intracellular recordings could be maintained for hours. As a number of compression and decompression cycles could be applied to a single cell without causing significant alterations in its excitable properties, we conclude that the mechanical damage inflicted to the neurons by local compression are reversible. Based on these observations, we suggest that the application of minimal local pressure or suction forces could be used to transform conventional extracellular field potential recordings into quasi-intracellular recording, and thereby dramatically improve both the signal to noise ratio and the quality of recordings from neurons cultured on CMOS semiconductors chips.

Keywords: Neuroelectronic hybrids; Floating gate transistor; Field potential; Action potentials; *Aplysia*

1. Introduction

The employment of standard CMOS technology to produce semiconductor chips for recording neuronal activity, or its future use to link neurons and transistors under *in vivo* conditions, suffers from a low signal to noise ratio (Offenhausser et al., 1997; Vassanelli and Fromherz, 1997, 1998). Experimental results and theoretical considerations have revealed that the signal to noise ratio is determined by three main factors: (a) the transistor's noise level (Arnaud and Galup-Montoro, 2003; Fleetwood et al., 2002); (b) the seal resistance formed between the neuron and the flat electrode surface (R_{seal}); (c) the intensity of the current generated by the neuron's activity (Cohen et al., 2006; Fromherz, 2003).

The current flow over R_{seal} can be either capacitive or Ohmic. The model developed by Fromherz and his colleagues (Fromherz, 2003) shows that when the membrane facing the transistor's gate (the junctional membrane) expresses a negligible number of voltage-independent ion channels, the FP is proportional to the first derivative of the intracellular voltage (Fromherz et al., 1991). If on the other hand, the junctional membrane is enriched by voltage-independent ion channels, the FP shape corresponds to that of the intracellular voltage (Fromherz et al., 1993; Jenkner and Fromherz, 1997). When the capacitive current is expressed by the ionic current through the non-junctional membrane, the FP is determined by the difference between the junctional and non-junctional membrane conductances (Fromherz, 1999).

* Corresponding author. Tel.: +972 2 6585091; fax: +972 2 5637033.
E-mail address: spira@cc.huji.ac.il (M.E. Spira).

0956-5663/$ – see front matter © 2007 Elsevier B.V. All rights reserved.
doi:10.1016/j.bios.2007.08.027

The value of R_{seal} is determined by the planar dimensions of the neuron–transistor junction and the width of the cleft formed between the plasma membrane and the device surface (Weis and Fromherz, 1997). Using optical methods and biophysical analysis, Braun and Fromherz (1998) and Zeck and Fromherz (2003) estimated that the cleft width formed between rat astrocytes cultured on silicon dioxide coated by laminin is approximately 100 nm. Accordingly, R_{seal} was estimated to be in the range of 1 MΩ (Weis and Fromherz, 1997). Electron microscopic analysis of thin sections prepared from cultured *Aplysia* neurons grown on 2D-polyaniline-coated glass substrate revealed that the cleft width ranges between hundreds of nm in some areas to 20–40 nm in others (Oren et al., 2004). It is generally accepted that a cleft dimension of 10–20 nm is the minimum width that can be formed by cells grown on substrates coated by biocompatible molecules (Sackmann and Bruinsma, 2002). Nevertheless, in practice R_{seal} can be increased either by enlarging the contact area formed between the neuron and the transistor-gate, or by reducing the average cleft width.

Consistent with the above, Jenkner and Fromherz (1997) reported that downward displacement of leech neurons cultured over transistors gate leads to an estimated increase in the seal resistance by a factor of ∼1.7 (from 2 to 3.5 MΩ). The vertical displacement of the neuron was also associated with a discrete increase in the junctional membrane conductance by approximately one order of magnitude (from 0.36 to 2.7 mS/cm^2). This switch, in concert with the increased seal resistance, led to a transformation of the field potential (FP) from a biphasic extracellular FP (proportional to the first derivative of the intracellular voltage), to a monophasic FP which resembles in shape intracellularly recorded action potential (Jenkner and Fromherz, 1997). The amplitudes of both the biphasic and monophasic FPs were increased by a factor of 2–5 (in the range of 1–5 mV). The discrete switch between the two modes of neuron–transistor coupling was attributed to alterations in the junctional membrane conductance imposed by the mechanical deformation of the cell body and its cytoskeleton which in turn affected ion channel conductances (Jenkner and Fromherz, 1997). The mechanical manipulation of cultured leech neurons, in respect to the sensing gate, inflicted mechanical damage to the neuron, and thus, repeated manipulations were rare. To the best of our knowledge, it is for this reason that this form of experimental manipulation was not reported again in the literature.

Using cultured *Aplysia* neurons grown on floating gate (FG) depletion type transistors, we extend here the pioneering studies of Jenkner and Fromherz (1997). We found that application of mechanical pressure on the cell body or axon of cultured *Aplysia* neurons gradually increased the seal resistance by increasing the contact area between the neuron and the gate surface and by reducing the average cleft width. As expected, this was associated with a gradual increase in the amplitude of the FP but was not associated with changes in its shape. With increased mechanical pressure, the capacitive coupling was transformed into an Ohmic coupling between the neuron and the transistor. Whereas the transformation appeared to be an all-or-none event, the mode of Ohmic coupling was stable for hours and the transformation could be repeated a number of times.

We conclude that high quality and hour-long recordings of action potentials can be obtained by pressing neurons against the flat sensing transistors pads. The principles described in the present study can be adopted to largely improve the quality of neuro-electronic coupling.

2. Materials and methods

2.1. The recording device

Depletion type P-channel floating gate MOS transistors with an octagonal sensing area of a diameter of 10 or 15 μm and W/L of 50/0.5 or 32/0.8 μm were designed and realized in a 0.5 μm CMOS technology, as described in an earlier study (Cohen et al., 2004). The geometrical separation between the octagonal sensing area and the transistor channel, allows for an optimal sensing area with respect to the neuron's dimensions, while realizing transistors with large transconductance (g_m). The poly-silicon floating electrode is placed between the gate oxide of 115 Å and the top oxide of 420 Å. The alteration in the FG electrode voltage modulates the transistor's drain-source current. This current is amplified by an external electronic system that filters the signal by a high-pass filter.

2.2. Materials

A marine species L-15 solution (msL-15): Leibovitz's L-15 Medium (Gibco-BRL, Paisley, Scotland) was supplemented according to Schacher and Proshansky (1983). Penicillin, streptomycin and amphotericin B (Biological Industries, Kibbutz Beit Haemek, Israel) were added up to final concentrations of 100 units/ml, 0.1 mg/ml and 0.25 μg/ml, respectively.

The culture medium consists of 5% filtered hemolymph, obtained from *Aplysia fasciata* (specimens collected along the Mediterranean coast) diluted in msL-15. Sulforhodamine 101 (SR101, Kodak) was prepared as a stock solution of 10 mM in double-distilled water (DDW), and further diluted before use in ASW to a final concentration of 40 μM.

2.3. Culture procedure

Left upper quadrant neurons (LUQ) from the abdominal ganglia of *Aplysia californica* were isolated and maintained in culture as previously described (Schacher and Proshansky, 1983; Spira et al., 1996, 1999). The neurons were plated on the chip's thermal oxide layer above the FG, which was coated with poly-L-lysine (Sigma, Rehovot, Israel). The experiments were performed 2–5 days after plating at room temperature (21–25 °C), and after replacing the culture medium with artificial sea water (ASW).

2.4. Confocal microscopy imaging

The system used for confocal imaging consisted of an Olympus microscope IX70 and a Bio-Rad Radiance 2000/AGR-3 confocal imaging system. The objective used was an Olympus planApo 60× 1.4 NA oil objective. In the experiment of Fig. 1,

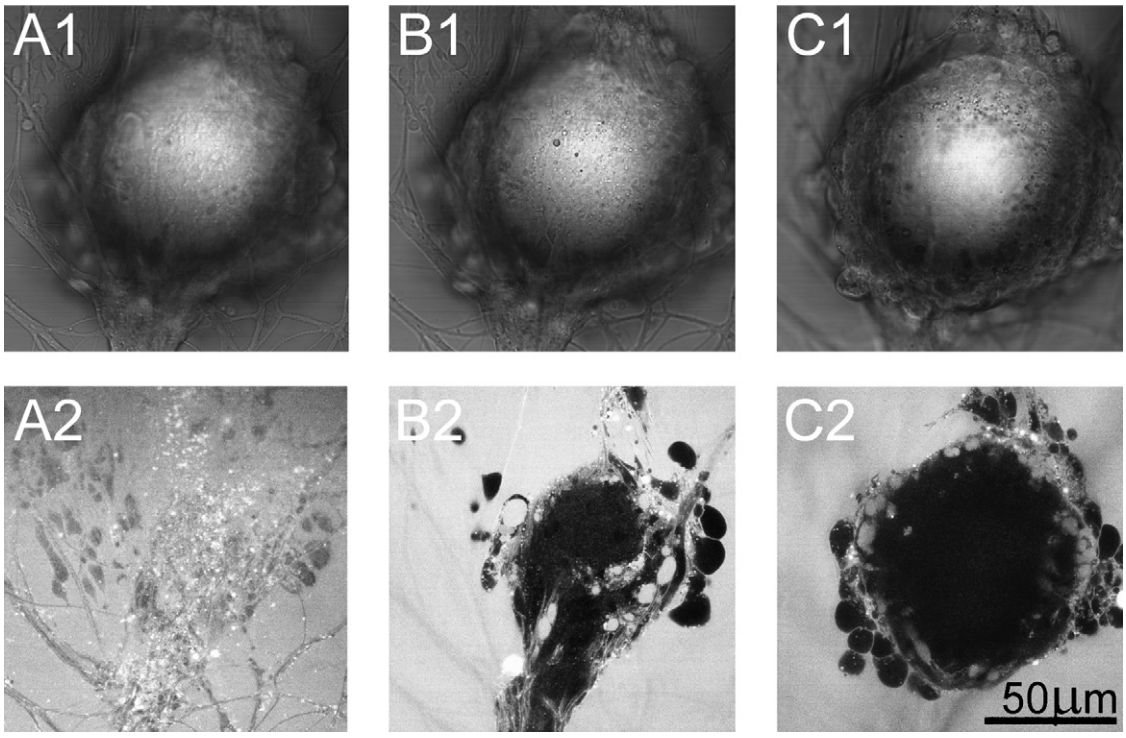

Fig. 1. Light and confocal microscope images of sulforhodamine removal from the cleft formed between the neuronal plasma membrane and the glass substrate as a consequence of minor mechanical pressure applied to the cell body. Twenty-four hours after plating, the hydrophilic fluorescent probe sulforhodamine (SR101) was added to the bathing solution. (A_1–C_1) are light micrographs of the cell body, in control (A1) and after application of minor mechanical pressure on the cell body (B_1, C_1). (A_2, B_2 and C_2) Confocal images taken at the level of the gap formed between the plasma membrane and the glass substrate. Note that as a consequence of pressure application, the SR101 solution is "squeezed out" of the gap, the fluorescent signal is reduced and the gap between the cell membrane and the substrate becomes darker. Likewise, as the pressure is increased, the dimensions of the dark area increase.

sulforhodamine was applied to the bathing solution and excited by a green HeNe laser of 543 nm wavelengths, and the emitted light was collected using the HQ 555–625 nm filter. Images were collected and processed using LaserSharp and LaserPix BioRad software, respectively. The figures were prepared using Adobe Photoshop and FreeHand software.

2.5. Electrophysiology

Conventional intracellular recording and stimulation with one or two microelectrodes were used. The microelectrodes were pulled from 1.5/1.02 mm borosilicate glass tubes with filaments, and filled with 2 M KCl. Electrode resistance ranged between 4 and 10 MΩ. For intracellular recording and stimulation, the microelectrode tip was inserted into the cell body.

2.6. Mechanical pressure

A micropipette was pulled from 1.5/1.02 mm borosilicate glass tubes and its tip was fire polished. The 10 μm polished micro-rod was guided by a micromanipulator to press the cell against the transistor sensing area under visual control. To evaluate the effect of applying mechanical pressure onto the cell body, we confocally imaged the fluorescent intensity of SR101 trapped within the gap between the plasma membrane poly-L-lysine-coated glass substrate. To that end, pressure was applied to the cell body of a neuron towards the substrate while imaging the fluorescent intensity (Fig. 1). The applied pressure increased the contact area between the cell body and the glass substrate while reducing the distance between them (Fig. 1).

2.7. Extracting transfer function between intracellular and extracellular voltages

Two intracellular electrodes were used: one for current injection and the other for intracellular voltage recording. Subthreshold sine wave currents with frequencies ranging between 1 Hz and 2 KHz were injected. The resulting intracellular and extracellular voltages were measured by the second intracellular microelectrode and the FG transistor, respectively (Fig. 2). Calculation of the voltages ratio recorded by the transistor to that of the intracellular one at various frequencies provided the transfer function of the neuroelectronic hybrid at these frequencies. At high frequencies, above 1 KHz, this ratio can be larger than 1 as a result of the attenuation of the intracellular signal by the time constant of the intracellular electrode.

2.8. Extracting of R_{seal} value, the neuron–transistor cleft width and the conductance of the junctional membrane

Similar to previous studies (Fromherz, 2003), the R_{seal} value, the neuron–transistor cleft width and the conductance of junctional membrane were calculated from the transfer function between intracellular and extracellular voltages. An example

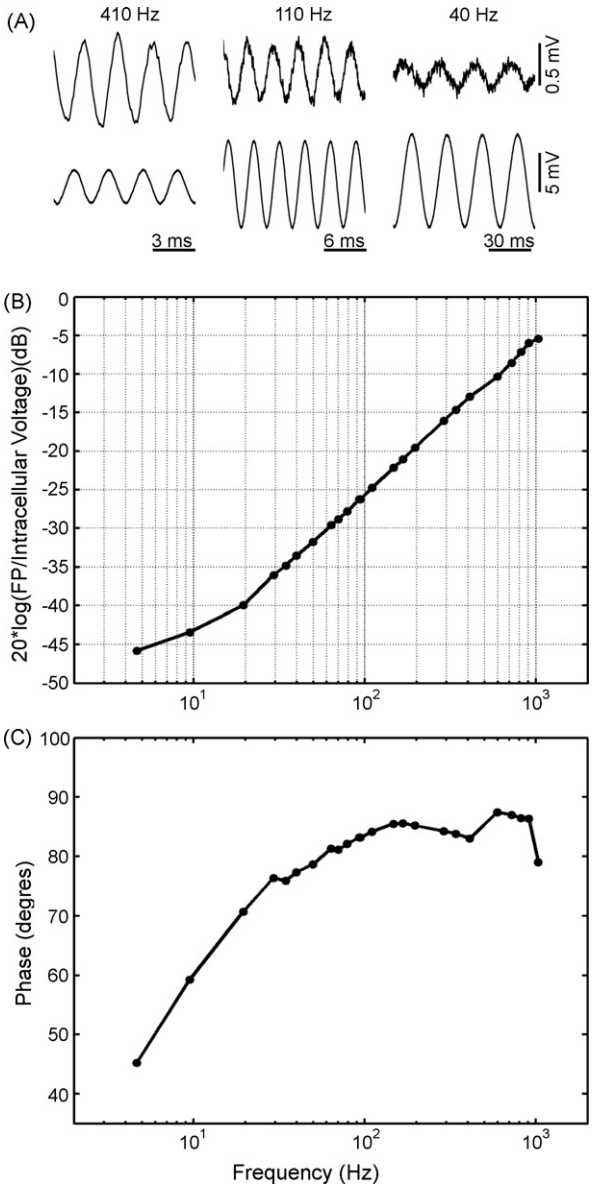

Fig. 2. Bode diagram of the amplitude ratios and phase between intracellular and extracellular measured voltage signals. (A) Samples of three pairs of sine waves voltage recordings at various frequencies. Intracellular voltage (lower traces) and extracellular voltage (upper traces). Every point in the Bode diagram (B and C) was extracted from such a pair of sine wave recordings. (B) The ratio of amplitudes between the extracellular voltage recorded by the transistor and the intracellular voltage. As expected from the theory of a system with one zero and one pole, the amplitudes ratios vs. the log of the frequency has a linear dependency at frequencies between the zero and the pole. (C) The phase between the extracellular voltage and the intracellular voltage.

is shown in Fig. 2. Briefly, the equivalent circuit parameters of the "point contact" model were fitted to the transfer function. In other cases, where the transfer function was not available, the following steps were taken to estimate the above parameters: (1) extracting the input resistance of the neuron from intracellular *I*/*V* curves. (2) Extracting the time constant and the membrane capacitance of the neuron membrane from the time response of the neuron membrane to a current step. (3) Extracting from these two parameters the total conductance of the neuron membrane. (4) Calculating cell area and estimating junctional area from microscopic images of the neuron. (5) Extracting the time constant of the neuron–transistor junction from the time response of the extracellular voltage recorded by the FG transistor. Then, calculating the resistance of junctional membrane (Rj) from knowing both the time constant and the membrane's capacitance. If it was not possible to extract the time constant of the junction due to low signal to noise ratio, we assumed a homogenous membrane conductance. (5) Extracting the ratio between extracellular and intracellular voltages (V_{extra}/V_{intra}) at a low frequency as shown in Fig. 2A. (6) Calculated the R_{seal} using Eq. (1).

$$\frac{V_{extra}}{V_{intra}} \cong \frac{R_{seal}}{R_j + R_{seal}}, \tag{1}$$

where V_{extra} is the extracellular voltage, V_{intra} is the intracellular voltage and R_j is the junction membrane resistance. (7) Calculating the neuron–transistor cleft thickness (d_j) using Eq. (2) (Fromherz, 2003).

$$d_j = \frac{\rho_j}{\pi \times \Phi \times R_j}, \tag{2}$$

where ρ_j is the specific resistance of the cleft, R_j is the junction membrane resistance and Φ is the scaling factor of the junction ($\Phi = 5$).

2.9. Simulation model

Simulations of action potentials, generated by a neuron composed of a cell body and an axon were conducted, using the "NEURON" multi-compartmental simulation model (Hines and Carnevale, 1997). The built-in extracellular mechanism ("insert extracellular") enabled us to simulate FPs generated outside the neuron. We constructed a neuron composed of a cell body with a diameter of 100 μm, and a cylindrical axon with a diameter of 20 μm. Hodgkin and Huxley (H&H) model was used to simulate the generation of action potentials (Hodgkin and Huxley, 1952). The default H&H parameters were resting potential of −70 mV, access resistance of 3.2 MΩ, maximum sodium conductance of 0.120 S/cm^2, maximum potassium conductance of 0.036 S/cm^2, leakage conductance of 0.003 S/cm^2 and the leakage reversal potential of −54.3 mV. The extracellular structure contained one extracellular layer and had the following parameters: (1) axial resistance (xraxial) of 10 MOhms/cm, (2) lateral conductance of 0.2 mho/cm^2 and (3) lateral capacitance of 0 μF/cm^2 (negligible capacitance of the floating gate electrode). All other parameters were taken from the H&H model.

3. Results

3.1. The characterization of neuron–transistor cleft dimensions

Two approaches were applied to characterize the dimensions of the cleft formed between cultured neurons and the device surface: electrical analysis of the transfer function between the

neuron and the transistor, and electron microscopic analysis (Oren et al., 2004).

An example of the electrophysiological approach is illustrated by Fig. 2. The cell body of a neuron cultured for 2 days over the sensing pad was impaled by two microelectrodes; one for current injection, and the other for voltage recordings. Subthreshold sine wave currents, with varying frequencies ranging between 1 Hz and 2 KHz were applied while recording the voltage drop across the plasma membrane. The generated FPs were concomitantly monitored by the intracellular microelectrode and the transistor (Fig. 2A). Bode's diagrams, revealing the amplitudes and the phase of the transfer function between the intracellular and the extracellular voltage recordings, are given in Fig. 2B and C, respectively. At high frequencies (>1 KHz), the ratio between extracellular and intracellular voltages is larger than 1. This is due to attenuation of the intracellular signal by the intracellular electrode time constant ($T = 0.16$ ms).

The R_{seal} extracted from the measurements shown in Fig. 2 is 1.65 MΩ (average 1.2 ± 0.43 MΩ, $n = 5$). Assuming that (i) the gap between the plasma membrane and the sensing electrode is homogeneous, (ii) the contact area has a radius of 40 μm and (iii) the resistivity of the physiological solution is 100 Ω cm, the width of the gap between the plasma membrane and the transistors surface in the experiment of Fig. 2, is estimated to be 38.5 nm (in 5 different experiments the estimated average gap width was 63 ± 36 nm). The estimated value of the cleft width from the above measurements is consistent with electron micrographs showing that the cleft width ranges between 20 and 100 nm (Oren et al., 2004).

We wish to note that we have not been able to perform the transfer function electrophysiological analysis while applying variable pressure on the cell body, since pressure application with two sharp microelectrodes in the cell leads to membrane rupture.

3.2. Increased seal resistance and junctional membrane conductance transfer capacitive to Ohmic coupling

3.2.1. Pressure applied to the cell body

For this experiment, the cell body of a LUQ neuron was cultured onto the surface of a FG transistor for 2 days (Fig. 3A). The neuron was then stimulated to fire action potentials by an intracellular microelectrode inserted into the soma. The evoked AP was recorded by the current injecting microelectrode using a bridge circuit (Fig. 3C_1 red), and extracellularly by the FG transistor (Fig. 3C'_1 black). Thereafter, mechanical pressure was applied onto the cell body by lowering a fire-polished glass rod mounted on a micromanipulator under visual control, and a coordinated adjustment of the intracellular microelectrode position. This resulted in gentle compression of the cell body against the FG surface (Fig. 3B). Increasing the pressure was associated with a small increase in the amplitude of the intracellular recorded AP, a slight increase in the neuron resting potential (from −47 mV in 3C_1 to −55.5 mV in 3C_3) and a slight decrease in the input resistance (from 12 to 11.3 MΩ). Concomitantly, the amplitude of the FP increased while maintaining its shape (Fig. 3C'_1–C'_3). The simultaneous increase in the transmembrane potential, increase AP amplitude and decrease in the input resistance are most likely due to pressure induced elevation in potassium conductance (Morris, 2001; Vandorpe and Morris, 1992; Vandorpe et al., 1994).

Further increase in the pressure leads to a decrease in the amplitude of the intracellular recorded AP (from 81 mV in C_3 to 65 mV in C_4) and an increase in its duration (Fig. 3C_4–C_5). These changes were associated with decreased trans-membrane potential from −51 mV (in 2C_4) to −30 mV (in 3C_5). These changes most likely reflect an increase in the conductance of the plasma membrane facing the floating gate pad. The mechanism underlying the increased membrane conductance could be related to the activation of "stretch-activated ion channels" (Morris, 2001; Vandorpe and Morris, 1992; Vandorpe et al., 1994), or to micro-holes of the plasma membrane facing the transistor's gate (McNeil and Kirchhausen, 2005; McNeil and Terasaki, 2001). These changes were associated with significant alterations in the FP shape from a complex FP to positively going, monophasic FP, and a tenfold increase in its amplitude and the signal to noise ratio (Fig. 3C_4–C_5). The recorded FP shape almost precisely overlapped the intracellular recorded action potential (compare Fig. 3C_4 and C'_4 and see Fig. 3D). When the mechanical pressure was released, the recorded monophasic FP gradually recovered its shape (Fig. 3C'_6–C'_7). Ten minutes after the release of the mechanical pressure, the recorded FP was still monophasic; only 20 min later, the FP resumed its original complex shape (Fig. 3C'_7). This slow recovery reflects the elastic properties of the cell, and the time required to recover the junctional membrane conductance.

The transformation of the FP from a low amplitude complex potential to a monophasic potential could be repeated a number of times suggesting that the damage inflicted to the plasma membrane is reversible. Furthermore, the experiment could be easily reproduced. We documented the phenomena in 12 successful experiments out of 17 attempts.

3.2.2. Pressure applied to the axon

The FP recorded from the cell body of cultured *Aplysia* neurons grown on a sensing pad is often composed in shape and is thus difficult to interpret. This reflects the fact that the cell body is only partially excitable and that several neurites extend from it. Thus, currents generated by spikes that propagate from the neurites into the cell body sum to generate complex FPs.

To simplify the observations and to examine whether the presumed micro-damages to the neuron is local, we extended the observations described above by examination of the transformation from capacitive to Ohmic coupling of an axonal segment (Fig. 4). For the experiment of Fig. 4, an action potential generated by intracellular stimulation of the cell body propagated along an axon, which was cultured on a FG electrode. The FP generated by a propagating action potential was characterized by a sharp downwards deflection (inward current, Fig. 4A). When mechanical pressure was applied to the axonal segment located just above the FG, the amplitude of the FP gradually increased (Fig. 4A1–A3). This was associated with the appearance of a positive going deflection preceding the inward current peak, representing outward current of the approaching AP, and a positive

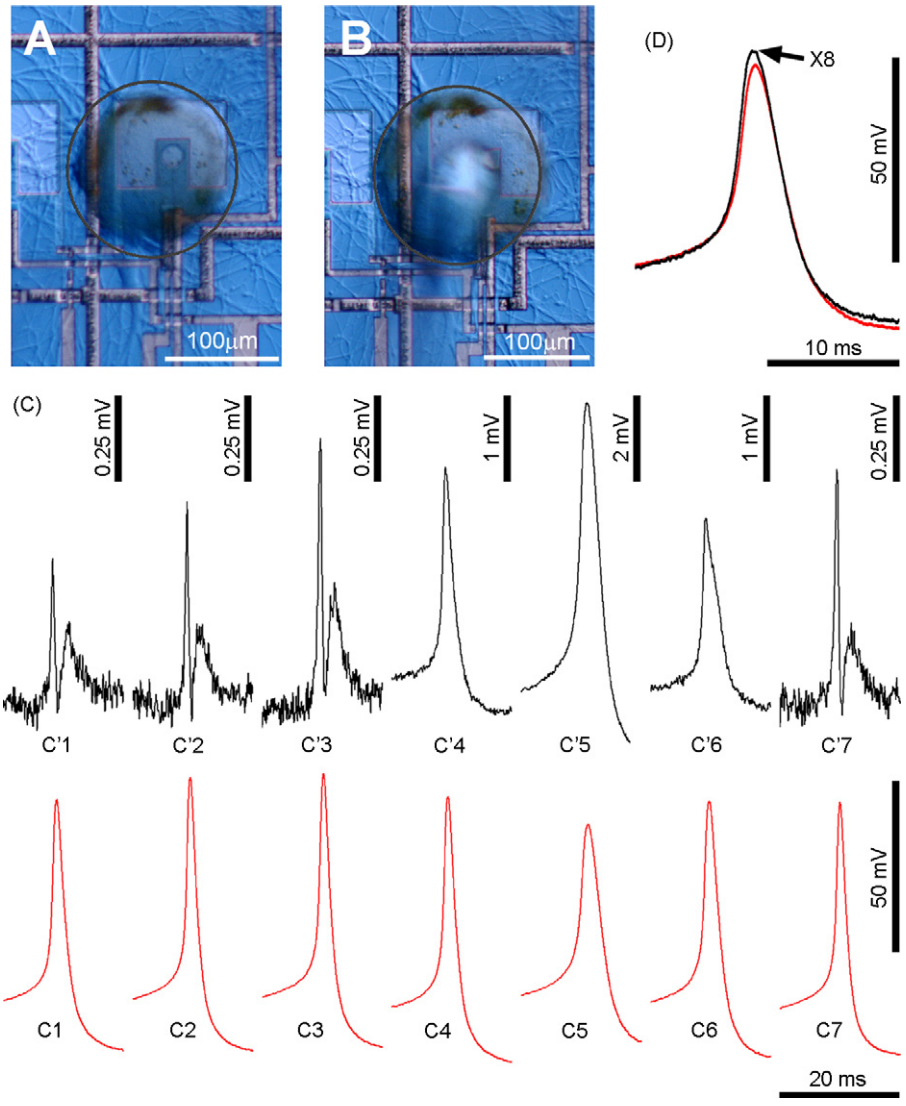

Fig. 3. The impact of mechanical pressure on the shape and amplitude of FPs recorded by a FG transistor. (A) LUQ neuron cultured on the surface of a FG transistor. (B) A smooth fire-polished glass rod compressed the cell body onto the chip surface. Note the slight increase in the diameter of the cell body as emphasized by the circles. (C) Intracellular voltage recordings in red, and FPs recordings by a FG transistor in black. The pressure was increased from C2 to C5 and then released (C5 to C7). (C1) Control—a complex FP. Increased mechanical pressure led to an increase in the amplitude of the FP but was not associated with a change in its shape (C′2–C′3). Further increase in the pressure transformed the FP into a monophasic FP resembling in its shape the intracellular recorded potential. (C6) Decreased amplitude of the monophasic FP was recorded 10 min after releasing the pressure from the cell body. After 20 min (C′7) the FP returned to its initial form (compare to C′1–C′3). Note the differences in the vertical scale bars in each trace, and that the amplitude of the intracellular voltage was decreased when the FP amplitude increased (for details see text). (D) Overlapping of the normalized intracellular recording (C5, red) and the FP (C′5, black).

hump after the peak inward current, representing back reflection of the "departing" AP (Fig. 4A1–A3). Further increase in the mechanical pressure transformed the shape of the FP from extracellular recording of the inward current to Ohmic recording of an attenuated intracellular potential with amplitude of 28 mV (Fig. 4A4). Concomitantly, the signal to noise ratio was increased by a factor of ∼100, from ∼3 to ∼300 (compare Fig. 4A1 and A4). As for the cell body, releasing the pressure led to gradual diminution of the AP amplitude recorded by the FG transistor. Since the shape of the potential was not altered, we concluded that whereas R_{seal} was reduced, the transistor was still Ohmically coupled to the neuron. With time, the Ohmic coupling reverted to capacitative coupling. Applying pressures once again led to an increase in the AP amplitude. Switching between capacitive to Ohmic recording could be repeated several times (Fig. 4A–C). As in the case of the cell body, the changes in the polarity and amplitude of the FP were associated with a decrease in the amplitude of the intracellular recorded action potential and a decrease in the trans-membrane potential. As described above, these changes are consistent with the assumption that the pressures led to increase in R_{seal} and junctional membrane conductance. Estimation of R_{seal} and the junctional membrane conductance as described above (Section 2.8), revealed that R_{seal} increased from 0.51 to 1.15 MΩ (Fig. 4C_1 and C_2), and the membrane conductance facing the sensing pad from 75 to 595 nS.

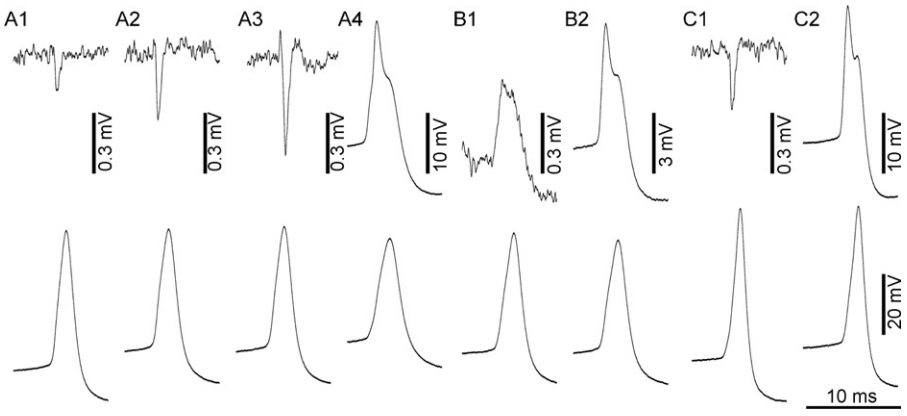

Fig. 4. The effect of mechanical pressure on the shape and amplitude of FPs generated by propagating action potential. For the experiment a neuron was cultured such that the axon adhered to the sensing pad. A microelectrode for both stimulation and recording was inserted into the cell body. To increase the contact area between the axon and the sensing pad and to reduce the cleft dimensions between the plasma membrane and the substrate surface a fire-polished glass rod pressed the axon downwards towards the sensing pad. The traces on the lower part are AP recorded by the intracellular electrode. On the upper part are the FPs recorded by FG transistor. Note, the different vertical scale bars of the recorded FPs. (A_1–A_3) Increasing the pressure applied to the axon lead to increase in the FPs amplitudes. (A_4) Further increase in the pressure transformed the FP from a 0.7 mV, negative going FP to about 20 mV positive action potential. This transformation is associated with a decrease in the action potential amplitude. (B_1) Releasing the pressure was associated with a marked decrease in the FP amplitude but not its shape and an increase in the intracellular recorded action potential. The process could be repeated several times. (C_1) Reduced pressure and (C_2) increased pressure. For further details, see text.

3.3. Computer simulation of the experimental results

To examine the interpretations of the results described above, we simulated the experimental protocol using the multi-compartment model—"NEURON" (Hines and Carnevale, 1997). For simulation, we used the default parameters of Hodgkin and Huxley (1952) for the squid giant axon. As the parameters defining the excitability of squid giant axons and *Aplysia* neurons differ, the simulation is expected to depict the qualitative trends of the experiments. For the simulation, we constructed a neuron composed of a cell body with a diameter of 100 μm, and a cylindrical axon with a diameter of 20 μm and length of 500 μm. The model neuron was "stimulated" by an intracellular depolarizing square pulse to the cell body, and "recording" the intracellular voltage from it (Fig. 5 red). The FPs were "recorded" by a 10 μm diameter "sensing pad" from the middle of the axon (Fig. 5 black). For the control simulation, the density of the voltage-gated channels of the cell body was chosen to be 50% of that of the axon. The propagating action potential along the axon generated a typical FP with a large negative peak representing the inward sodium current (Fig. 5A black trace). In a series of simulations in which the seal resistance was increased, or the membrane conductance of the membrane patch facing the sensing pad was deceased, we found that over a large

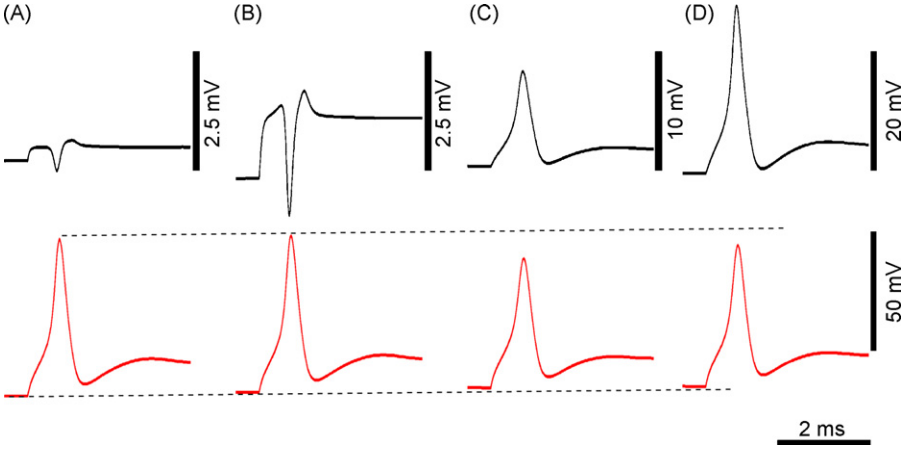

Fig. 5. Computer simulations of action potentials recorded by an intracellular microelectrode and FPs generated by a propagating action potential in control, and after "application of pressure" onto the axonal segment located above the sensing pad. The simulated neuron is composed of a cylindrical cell body with a diameter of 100 μm, an axon with a diameter of 20 μm and length of 500 μm. The simulation was generated by delivering an intracellular depolarizing square pulse to the cell body, and "recording" the action potential by the intracellular electrode (red) and the FPs from the middle of the axon (black). (A) A control simulation—negative FP was recorded. (B) Increasing the seal resistance under the axon by a factor of 5 with respect to the controlled lead to an increase in the FP amplitude but did not alter its shape. Likewise the shape and amplitude of the intracellularly recorded AP did not change. (C) The leak conductance of the membrane above the electrode was increased by a factor of 16 with respect to the control. This leads to the transfer of the negative FP to a positive one. (D) Increasing both the seal resistance under the axon by a factor 5, and the leak conductance of the axonal membrane above the electrode by a factor of 16 leads to an increase in the amplitude of the FP to 30 mV.

range of alterations the model depicted the experimental results. To illustrate the results, we present in Fig. 5, the outcome of increasing the seal resistance under the axon by a factor of 5 (Fig. 5A and B, black) and the leak conductance of the membrane facing the sensing electrode by a factor of 16 (Fig. 5C). Whereas increasing R_{seal} by $\times 5$ led to an increase in the simulated FP amplitude without alteration in its shape, increasing the leak conductance of the membrane by a factor of 16 (without altering the seal resistance) switched the shape of the FP from a negative to a positive going monophasic FP (Fig. 5C black) concomitantly with a decrease in the amplitude of the intracellular "recorded" action potential. The combination of increasing the seal resistance by a factor of 5, and increasing the membrane leak conductance above the electrode by a factor of 16, resulted in recording an action potential with an amplitude of about 30 mV (Fig. 5D black). As in the experiments the "recorded" FP under these conditions is similar in its shape to that of the intracellular voltage.

4. Discussion

The main findings of the present study are that mechanical pressure applied to restricted neuronal compartment induces a reversible local increase in the junctional membrane conductance associated with increased R_{seal}. This transfers the capacitive coupling between the neuron and the transistors on which it was grown to Ohmic coupling. Under such conditions a semi-intracellular AP with an amplitude of up to 30 mV can be recorded. We estimated that the moderate pressure applied to the neuron increased the seal resistance from ~0.5 to ~1.2 MΩ, and induced an increase in the junctional membrane conductance from 75 to ~600 nS. Since we have been able to maintain the semi-intracellular recordings for several hours, and transfer capacitative FP recordings to Ohmic semi-intracellular recordings a number of times, we conclude that the mechanical damages inflicted to cultured *Aplysia* neurons by local compression are reversible.

Our basic observations are consistent with the pioneering study of Jenkner and Fromherz (1997). We attribute the differences in the values of coupling coefficients obtained in the two studies and the tolerability of the neurons to the mechanical manipulations to differences in the preparations used for the experiments.

The nature of changes in the FP amplitude and shape with increased pressure suggests that two independent mechanisms are involved: (a) pressure induced increase in the FPs amplitude without a significant change in its shape. This change reflects the increase in the seal resistance formed between the neurons plasma membrane and the device surface. (b) The switch in the FP shape from biphasic (Figs. 3–5) to monophasic is attributed, as suggested by Jenkner and Fromherz (1997), to an increase in the conductance of the plasma membrane facing the FG. Since we observed an increase or decrease in the amplitudes of either biphasic potentials or monophasic potential while applying and releasing the mechanical pressure, we concluded that the two mechanisms may operate independently of each other.

Due to technical difficulties, we could not monitor and calculate the seal resistance using sub-threshold sine wave analysis while applying and releasing the pressure. Based on imaging of the fluorescent signal intensity generated by a hydrophilic probe (SR101) trapped in between the cell's plasma membrane and the substrate we attributed the increased R_{seal} to increased contact area between the plasma membrane and the FG surface and reduction in the averaged cleft width (Fig. 1). We recall that in earlier electron micrographs from our laboratory, we documented a narrow cleft of 20–40 nm in some areas of contact while in other locations the cleft width is significantly larger (Oren et al., 2004).

The quantitative change in the FP shape from biphasic to monophasic (Figs. 3–5) is attributed as suggested by Jenkner and Fromherz (1997) to increase in the conductance of the plasma membrane facing the FG. This could be due to either the activation of stretch-dependent channels expressed on the plasma membrane that face the FG surface (Morris, 2001; Vandorpe and Morris, 1992; Vandorpe et al., 1994), or to the formation of non-specific injury pores at the plasma membrane facing the gate (McNeil and Kirchhausen, 2005; McNeil and Terasaki, 2001). Since the kinetics of activation and inactivation of stretch-activated ion channels of *Aplysia* neurons is very short compared with our observations (in the range of milliseconds to hundred of milliseconds, Vandorpe et al., 1994) we tentatively suggest that the injury pores are formed by the deformation of the junctional plasma membrane. We attribute the slow (minutes long), recovery of the FP after releasing the pressure to the time needed for the cascade of cellular events leading to membrane repair (McNeil and Kirchhausen, 2005; McNeil and Terasaki, 2001). An increase in membrane conductance illustrated in the experiment of Fig. 4 is equivalent to the creation of a single pore with diameter of 15 nm.

Whatever the mechanisms of increased membrane conductance are, we conclude that under these conditions the cytoplasm comes into direct Ohmic contact with the gate surface, and thus the shape of the recorded potential is similar to that elicited by intracellular recording (Figs. $3C_4$, $4B_2$ and 5D).

As it stands, the on-cell mechanical pressure application, demonstrated in the present study cannot be used as a routine tool to study neuronal networks grown on a matrix of flat electrodes. Nevertheless, the principles can be adopted and developed to largely improve the quality of neuro-electronic coupling.

The classical patch-clamp technique of Neher and Sakmann (Neher and Sakmann, 1976, 1992; Sakmann and Neher, 1984) was recently adapted to on-chip patch-clamp configuration. These devices make use of micro-fabricated structures particularly designed to patch clamp suspended cells that are sucked into a "micropipette" (Li et al., 2006; Pantoja et al., 2004; Sordel et al., 2006). The method could not be applied so far to study adhered neurons that grew on a defined substrates (Jung et al., 2001; Nisbet et al., 2006). Based on the present results, it is conceivable that the use of minimal suction may be sufficient to generate high R_{seal} and create the nano-pores in the cell membrane to allow intracellular recordings from hundreds of cells.

5. Conclusions

Recordings of the electrical activity generated by neurons cultured on semiconductor chips suffer from low signal to noise ratio. This can be significantly improved by a slight increase in the seal resistance formed between the neuron membrane and the substrate and increase conductance of the plasma membrane facing the transistors sensing pad. These alterations can be achieved by slight mechanical pressure or by suction applied to restricted and relevant neuronal compartment, and culminate in the transfer of capacitive coupling between neurons and transistors to Ohmic coupling.

Acknowledgements

This study was supported by a grant from the Future and Emerging Technologies arm of the 5th and 6th IST Programme (No. IST-1999-29091, and IST-510574). Parts of the study were carried out at the Charles E. Smith Family and Prof. Joel Elkes Laboratory for Collaborative Research in Psychobiology. The Neuro-Electronic research group of M.E.S., J.S., and S.Y. was established in 2000 by funding from the Israel Ministry of Science. Funding of this project was refused by the Israel Science Foundation. M.E. Spira is the Levi DeViali Professor in Neurobiology.

References

Arnaud, A., Galup-Montoro, C., 2003. IEEE Trans. Electron Devices 50, 1815–1818.
Braun, D., Fromherz, P., 1998. Phys. Rev. Lett. 81, 5241–5244.
Cohen, A., Shappir, J., Yitzchaik, S., Spira, M.E., 2006. Biosens. Bioelectron. 22, 656–663.
Cohen, A., Spira, M.E., Yitshaik, S., Borghs, G., Shwartzglass, O., Shappir, J., 2004. Biosens. Bioelectron. 19, 1703–1709.
Fleetwood, D.M., Xiong, H.D., Lu, Z.Y., Nicklaw, C.J., Felix, J.A., Schrimpf, R.D., Pantelides, S.T., 2002. IEEE Trans. Nucl. Sci. 49, 2674–2683.
Fromherz, P., 1999. Eur. Biophys. J. 28, 254–258.
Fromherz, P., 2003. In: Waser, R. (Ed.), Nanoelectronics and Information Technology. Wiley-VCH Verlag, Berlin, pp. 781–810.
Fromherz, P., Muller, C.O., Weis, R., 1993. Phys. Rev. Lett. 71, 4079–4082.
Fromherz, P., Offenhausser, A., Vetter, T., Weis, J., 1991. Science 252, 1290–1293.
Hines, M.L., Carnevale, N.T., 1997. Neural Comput. 9, 1179–1209.
Hodgkin, A.L., Huxley, A.F., 1952. J. Physiol. Lond. 117, 500–544.
Jenkner, M., Fromherz, P., 1997. Phys. Rev. Lett. 79, 4705–4708.
Jung, D.R., Kapur, R., Adams, T., Giuliano, K.A., Mrksich, M., Craighead, H.G., Taylor, D.L., 2001. Crit. Rev. Biotechnol. 21, 111–154.
Li, X., Klemic, K.G., Reed, M.A., Sigworth, F.J., 2006. Nano Lett. 6, 815–819.
McNeil, P.L., Kirchhausen, T., 2005. Nat. Rev. Mol. Cell. Biol. 6, 499–505.
McNeil, P.L., Terasaki, M., 2001. Nat. Cell. Biol. 3, E124–E129.
Morris, C.E., 2001. Cell. Mol. Biol. Lett. 6, 703–720.
Neher, E., Sakmann, B., 1976. Nature 260, 799–802.
Neher, E., Sakmann, B., 1992. Sci. Am. 266, 44–51.
Nisbet, D.R., Pattanawong, S., Nunan, J., Shen, W., Horne, M.K., Finkelstein, D.I., Forsythe, J.S., 2006. J. Colloid Interface Sci. 299, 647–655.
Offenhausser, A., Sprossler, C., Matsuzawa, M., Knoll, W., 1997. Biosens. Bioelectron. 12, 819–826.
Oren, R., Sfez, R., Korbakov, N., Shabtai, K., Cohen, A., Erez, H., Dormann, A., Cohen, H., Shappir, J., Spira, M.E., Yitzchaik, S., 2004. J. Biomater. Sci. Polym. Ed. 15, 1355–1374.
Pantoja, R., Nagarah, J.M., Starace, D.M., Melosh, N.A., Blunck, R., Bezanilla, F., Heath, J.R., 2004. Biosens. Bioelectron. 20, 509–517.
Sackmann, E., Bruinsma, R.F., 2002. Chem. Phys. Chem. 3, 262–269.
Sakmann, B., Neher, E., 1984. Annu. Rev. Physiol. 46, 455–472.
Schacher, S., Proshansky, E., 1983. J. Neurosci. 3, 2403–2413.
Sordel, T., Garnier-Raveaud, S., Sauter, F., Pudda, C., Marcel, F., De Waard, M., Arnoult, C., Vivaudou, M., Chatelain, F., Picollet-D'hahan, N., 2006. J. Biotechnol. 125, 142–154.
Spira, M.E., Dormann, A., Ashery, U., Gabso, M., Gitler, D., Benbassat, D., Oren, R., Ziv, N.E., 1996. J. Neurosci. Methods 69, 91–102.
Spira, M.E., Gitler, D., Oren, R., Ziv, N.E., 1999. In: Haynes, L.W. (Ed.), The Neuron in Tissue Culture. John Wiley and Sons Ltd, pp. 87–103.
Vandorpe, D.H., Morris, C.E., 1992. J. Membr. Biol. 127, 205–214.
Vandorpe, D.H., Small, D.L., Dabrowski, A.R., Morris, C.E., 1994. Biophys. J. 66, 46–58.
Vassanelli, S., Fromherz, P., 1997. Appl. Phys. A: Mater. Sci. Process. 65, 85–88.
Vassanelli, S., Fromherz, P., 1998. Appl. Phys. A: Mater. Sci. Process. 66, 459–463.
Weis, R., Fromherz, P., 1997. Phys. Rev. E 55, 877.
Zeck, G., Fromherz, P., 2003. Langmuir 19, 1580–1585.